DETECTION AND CLASSIFICATION OF SINGLE LINE TO GROUND BOUNDARY FAULTS IN A 138 KV SIX PHASE TRANSMISSION LINE USING HILBERT HUANG TRANSFORM

By

GAURAV KAPOOR

Assistant Professor, Department of Electrical Engineering, Modi Institute of Technology, Rajasthan Technical University, Rawatbhata Road, Nayagaon, Kota, Rajasthan, India.

Date Received: 25/12/2018 Date Revised: 05/06/2019 Date Accepted: 22/06/2019

ABSTRACT

In this study, a fault detection technique and faulty phase identification technique using Hilbert Huang Transform (HHT) are presented for single line to ground boundary faults in six phase transmission line. Hilbert Huang transform is used for processing of the six phase fault current signals, which are recorded by the transducers located at bus-1 of the six phase transmission line. The possibility of the HHT-based fault detection technique is tested under the variation of fault type, fault location, fault inception time, fault and ground resistances.

Keywords: Boundary Fault Detection, Faulty Phase Identification, Hilbert Huang Transform, Six Phase Transmission Line Protection.

INTRODUCTION

Latest era have observed an increase in the necessity of electricity and to assist the increasing need of electricity, the power transfer ability of active transmission network should be boosted. Higher phase order (six phase) transmission lines have been proposed as a prospective substitute which have the potential to transfer the large amount of electrical power with no chief adaptation in the current configuration of power transmission system.

Owing to the connection of great number of conductors, the likelihood of occurrence of fault in six phase transmission line is more. Thus, it is also crucial to develop a satisfactory protection technique, which would decide the faulty phase to drop off the restoration period and therefore improve the consistency of the power transmission system. The larger number of feasible fault combinations in six phase transmission line makes the difficulty of fault detecting/classifying the faults very complicated. A number of prominent works have been reported in the literatures on the topics related to the protection and economics of six phase transmission lines which are described hereafter. Shunt faults detection and classification in six phase transmission line using a combination of artificial neural network and wavelet transform has been presented by (Koley, Verma, & Ghosh, 2017). Sharma, Ali, & Kapoor (2018) used mathematical morphology for the boundary protection of six phase transmission line. Detection and classification of open conductor faults in six phase transmission line using a combination of discrete Fourier transform and k-nearest neighbour has been reported in (Shukla & Koley, 2017). Phase to phase fault detection in series capacitor compensated six phase transmission line using the norm of wavelet transform has been presented in (Kapoor, 2018f). In (Kapoor, 2018e), discrete wavelet transform has been utilized for the detection and classification of simultaneously occurring single phase to ground faults and open conductor faults in a twelve phase transmission line compensated with series capacitor. Discrete Fourier transform in combination with fuzzy inference system has been used as a very helpful tool for fault detection and classification of shunt faults in six phase transmission line (Ashok & Yadav, 2018). Investigation of TCSC connected multi-phase (6-phase and 12-phase) transmission line is presented in (Tripathi & Bhardwaj, 2014). Further, protection scheme based on the combination of artificial neural network and wavelet transform has been developed for protection against shunt faults in six phase transmission line (Kumar, Koley, Yadav, & Thoke, 2014). In (Zhipeng, Pingping, Zheng, & Zhu, 2012), a method of decoupling is proposed for a four circuit (12-phase) transmission line fault analysis. A twelve sequence component method has also been used for fault location in twelve phase transmission line (Fan, Liu, & Tan, 2011). Open conductor fault calculation in a twelve phase transmission line having four circuits using a twelve sequence component method has been reported in (Peng, Gang, Haifeng, Yuansheng, & Pu, 2010). Power flow and stability analysis has been carried out on a six phase and twelve phase transmission lines and has been reported in (Husain, Singh, & Tiwani, 2007). In (Demir, Kilic, & Ozbey, 1998), phase coordinate method has been applied for the load flow analysis of integrated three phase and multi-phase (6-phase and 12-phase) transmission lines. In (Dorazio, 1990), researchers determined the economic value of higher phase order transmission line and compared it with the conventional three phase power transmission system. In (Binsaroor & Tiwari, 1988), analytical expressions are derived and evaluated for the transmission line parameters of a 12-phase transmission system considering transposed and un-transposed conditions of a 12-phase transmission line.

Recently, the protection of multi-phase power transmission lines has engaged much consideration from researchers and very less research has been done on six phase transmission line protection. A fault can take place at various locations on six phase transmission line and in different phases. The conventional protection techniques used to protect the six phase transmission line against shunt faults, which occur at various locations are not able to detect/ classify the faults which occur at the boundary of six phase transmission line. Current research has been focused on the protection of six phase power transmission line against a variety of single line to ground faults, which occur at the boundaries of six phase transmission line by the usage of Hilbert Huang transform based approach which according to author no one did this before in the past.

1. Specifications of Six Phase Transmission Line

The schematic of the six phase transmission line is shown in Figure 1. The six phase power system consists of a 138 kV, 60 Hz, 68 km long six phase transmission line, separated into two sections. Each section has a length of 34 km. The six phase transmission line is fed from a 138 kV source at the sending and receiving end. Two loads of 300 MW and 150 MVAr are connected at the receiving end of a six phase transmission line. The proposed six phase transmission line test system is developed and simulated using the simscape power system toolbox of MATLAB.

As exemplified in Figure 1, the relay is connected at bus-1 to protect the entire six phase transmission line. The six phase pre-fault current (I_A, I_B, I_C, I_D, I_E, I_F) and voltage (V_A, V_B, V_C, V_D, V_E, V_F) waveforms of corresponding phases are shown in Figure 2. Figure 3 depicts the Hilbert Huang coefficients of six phase current during the no-fault condition. Table 1 shows the response of the proposed technique during the no-fault condition.

2. Hilbert Huang Transform and Proposed Protection Technique

The Hilbert transform for a test signal f(t) is defined as given in equation (1) below:

$$H\{f(t)\} = -\frac{1}{\pi}\int_{-\infty}^{\infty} f(\tau)\frac{d\tau}{\tau - t} = -\frac{1}{\pi t} * f(t) \qquad (1)$$

Hilbert transform can be defined as the convolution between f(t) and $-1/\pi t$.

This equation defines an inappropriate integral because for t = τ, the integral has an exceptionality. So the integral is calculated symmetrically to avoid this difficulty.

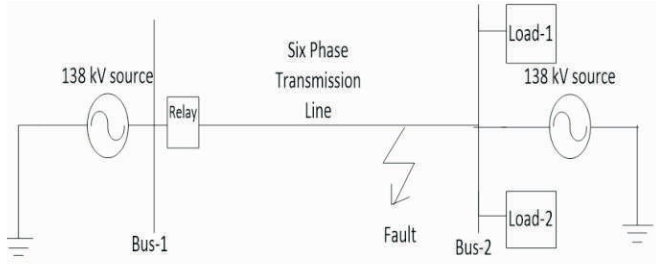

Figure 1. Single Line Diagram of Series Compensated Six Phase Transmission Line under Study

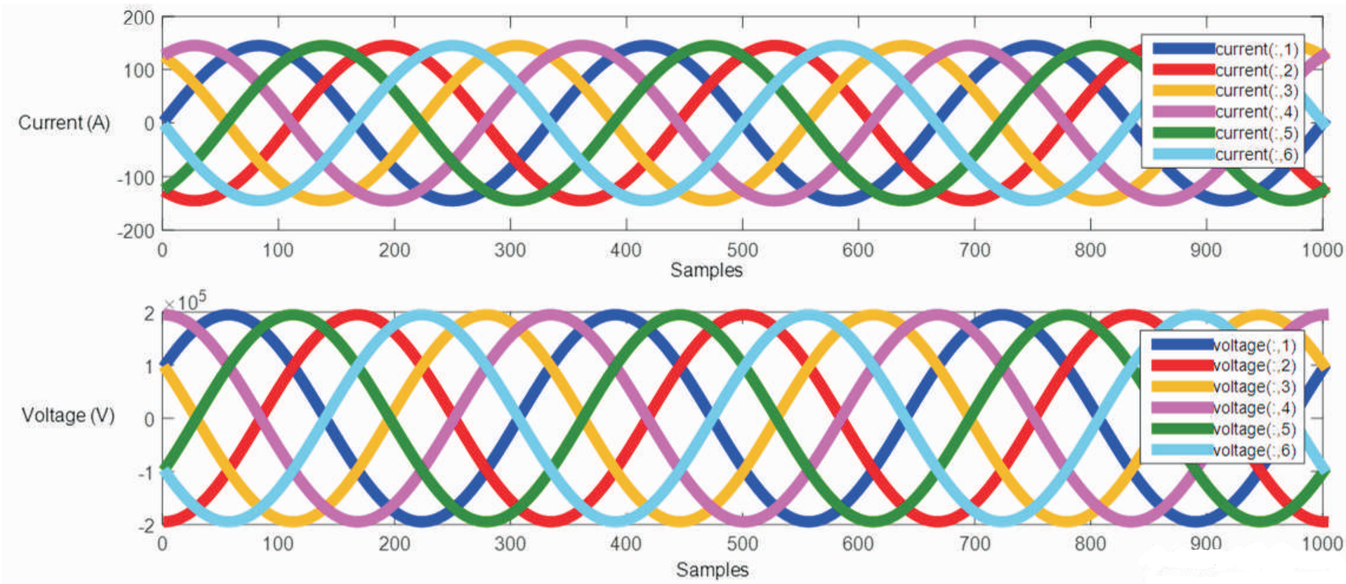

Figure 2. Six Phase Current and Voltage Waveform during No-fault

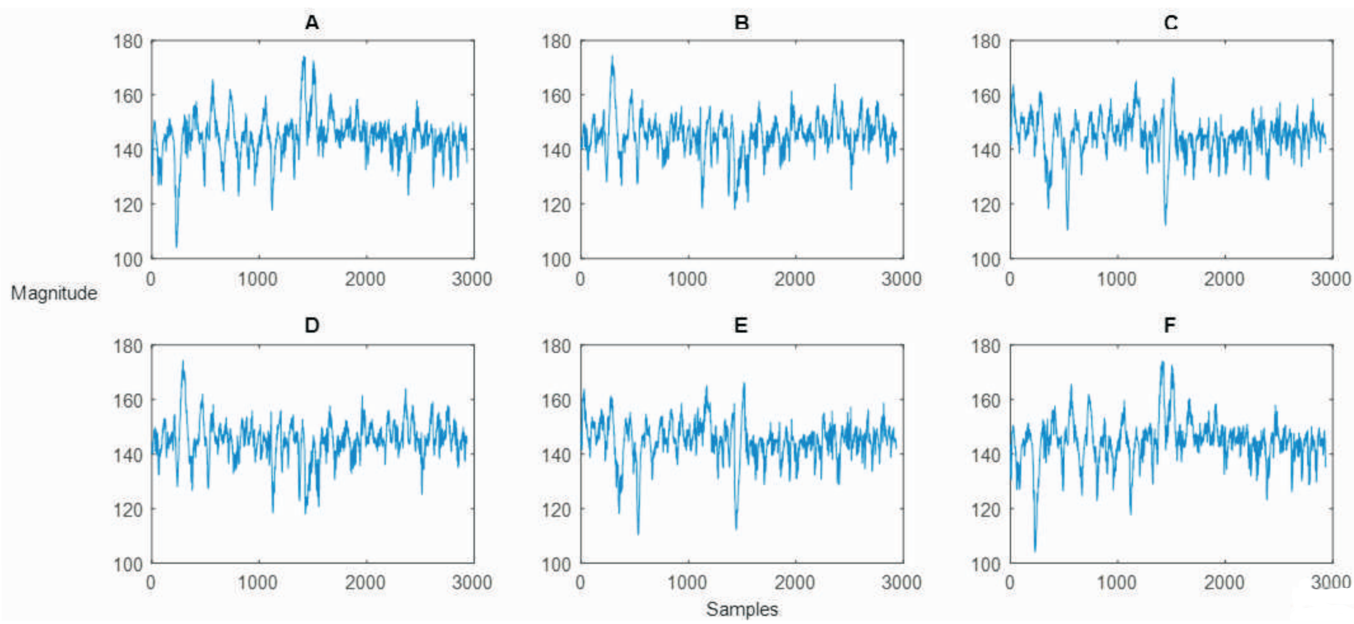

Figure 3. Hilbert Huang Transform Coefficients of Six Phase Current during No-fault

Phase	Hilbert Huang Transform Coefficients
A	174.2376
B	174.3952
C	166.3926
D	174.4135
E	166.3862
F	174.2411

Table 1. Test Result for No-fault

$$\int_{-\infty}^{\infty}\frac{g(\tau)}{t-\tau}d\tau = \lim_{e\to 0}\left[\int_{-\infty}^{t-e}\frac{g(\tau)}{t-\tau}d\tau + \int_{t+e}^{\infty}\frac{g(\tau)}{t-\tau}d\tau\right] \quad (2)$$

Inverse Hilbert transform can be deliberated by equation (3), where g' (t) and g (t) are part of pair transform of Hilbert.

$$g(t) = -\frac{1}{\pi}\int_{-\infty}^{\infty}\frac{g'(t)}{t-\tau} * d\tau \quad (3)$$

From the definition of Hilbert Transform it is observed that g'(t) can be understood as the convolution of g(t) with the signal -1/πt.

$$g'(t) = g(t) * \frac{1}{\pi t} \quad (4)$$

Step 1: Simulate the six phase test system and generate post fault six phase current signals.

Step 2: Analyze the six phase current signals using Hilbert Huang transform for features extraction.

Step 3: Calculate the magnitude of Hilbert Huang coefficients for each phase fault current signal.

Step 4: If the magnitude of Hilbert Huang coefficients of the faulted phase is greater than the magnitude of Hilbert Huang coefficients of un-faulted phase, then fault occurs else no fault, go to step 1.

Figure 4 shows the proposed fault detection and faulty phase identification technique.

3. Performance Evaluation

To validate the efficacy of the proposed fault detection/ classification technique, test studies have been approved for various types of single line to ground boundary faults. The consequence of variation in fault type (FT), fault location (FL), fault inception time (FIT), fault resistance (RF), and ground resistance (RG) has been examined. Following

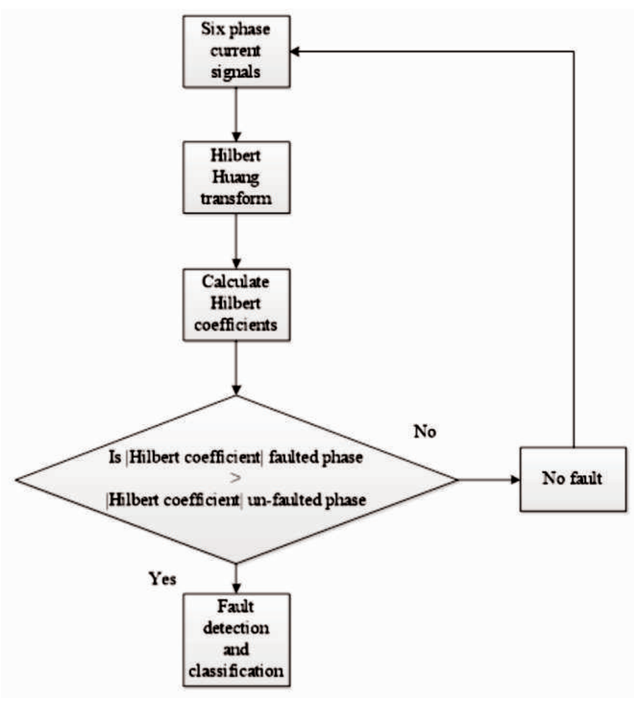

Figure 4. Proposed Fault Detection and Faulty Phase Identification Technique

the single line to ground fault detection/ classification technique, few simulation results are discussed in the successive subsections.

3.1 Performance in Case of AG near-end Fault: Case-I

The response of the proposed technique is tested for AG single line to ground fault when the AG fault is triggered at a distance of 2 km near to the relaying point at fault inception time of 0.04 seconds with RF = 3 Ω and RG = 6 Ω. Figure 5 demonstrates the waveform of six phase current when the six phase transmission line is subjected to AG fault at a distance of 2 km near to the relay location at FIT = 0.04 seconds. Figure 6 shows the procedure of feature extraction using the Hilbert Huang transform for six phase current during AG fault. Figure 6 depicts the Hilbert Huang transform coefficients of six phase current during AG fault at a distance of 2 km from the relaying point. As observed in Figure 6, the Hilbert Huang coefficient of phase A has a higher magnitude in comparison to the magnitudes of Hilbert Huang coefficients of other phases conforming that the fault type is AG fault on six phase transmission line with phase-A as the faulty phase. It can also be seen from Figure 6 that the HHT coefficient of phase-A has a lower magnitude of noise content in comparison to the noise content of HHT coefficients of other phases. This is due to the fact that the AG fault is a near-end fault, which is simulated at a distance of 2 km from bus-1 on six phase transmission line. Table 2 depicts the response of proposed fault detection and classification technique for AG fault. It is clear from Table 2 that the proposed technique detects and classifies the fault correctly, for AG fault occurring very near to the relaying point of six phase transmission line.

3.2 Performance in Case of BG near-end Fault: Case-II

The performance of the proposed technique is evaluated for BG single line to ground fault when the BG fault is triggered at a distance of 4 km near to the relay location at fault inception time of 0.16 seconds with RF = 6 Ω and RG = 9 Ω. Figure 7 demonstrates the waveform of six phase current when the six phase transmission line is subjected to BG fault at 4 km away from the relay location at FIT = 0.16 seconds. The process of feature extraction using the Hilbert Huang transform for six phase current during BG fault is

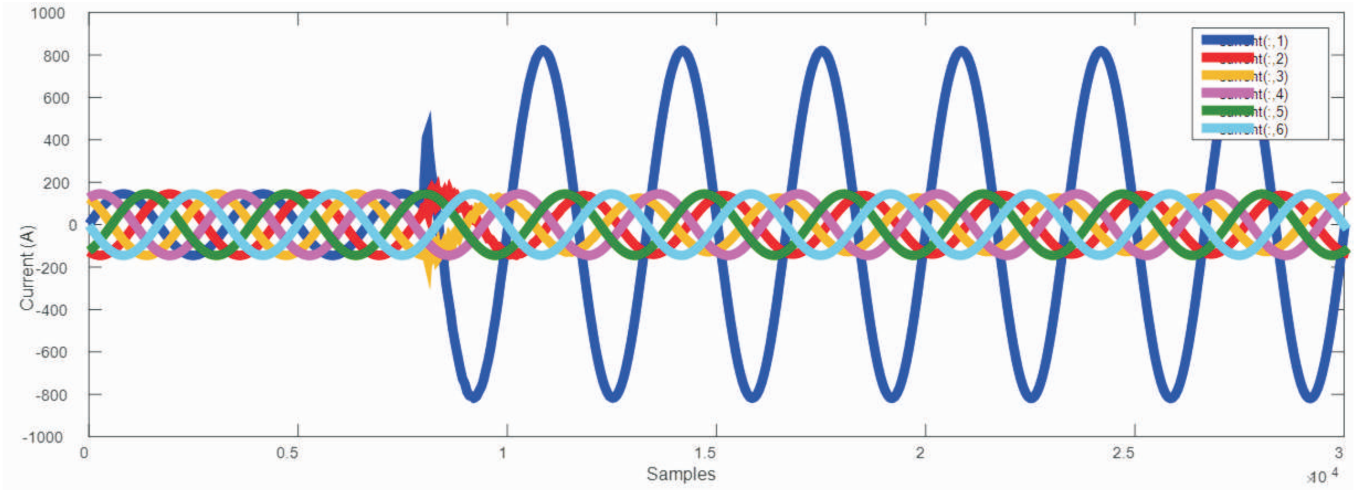

Figure 5. Six phase Current during AG Fault at FIT=0.04 seconds at 2 km from bus-1 with RF = 3 Ω and RG = 6 Ω

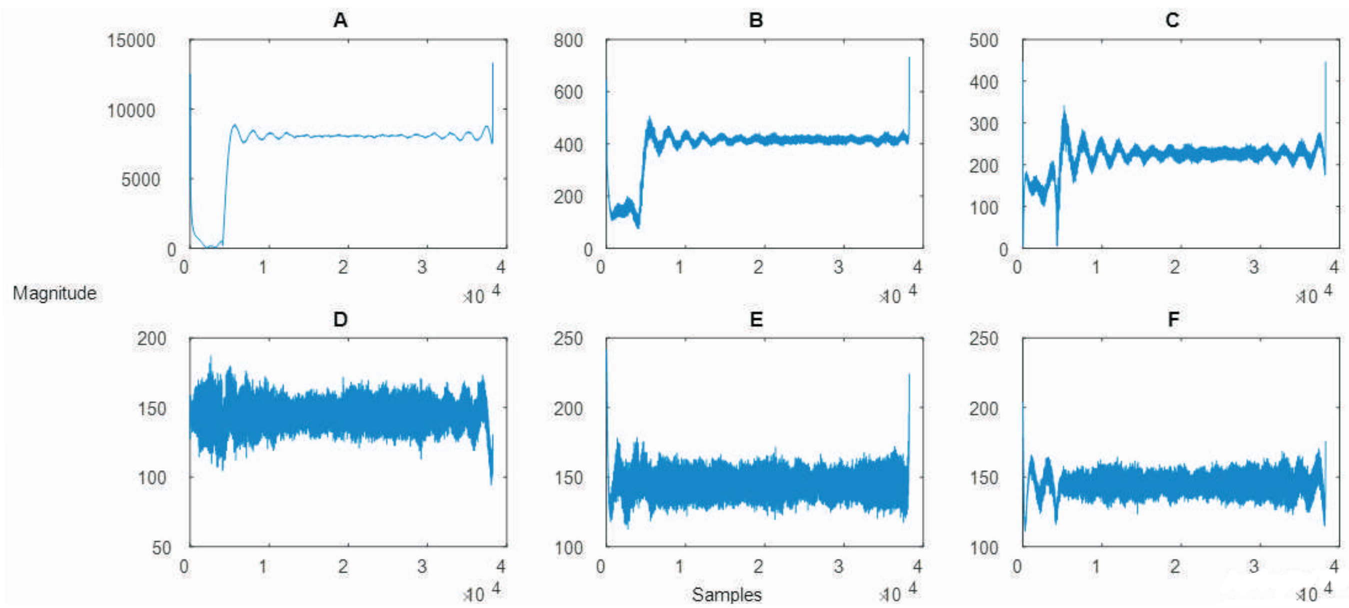

Figure 6. Hilbert Huang transform coefficients of six phase current during AG fault at FIT=0.04 seconds at 2 km from bus-1 with RF = 3 Ω and RG = 6 Ω

Phase	Hilbert Huang Transform Coefficients
A	1.3306*10^4
B	732.3584
C	446.4299
D	187.3232
E	241.9698
F	203.6433

Table 2. Test Result for AG Fault at 2 km at FIT = 0.04 seconds with RF = 3 Ω and RG = 6 Ω

depicted in Figure 8. Figure 8 shows the Hilbert Huang transform coefficients of six phase current during BG fault at a distance of 4 km from the relaying point. As can be seen from Figure 8, the Hilbert Huang coefficient of phase B has a higher magnitude in comparison to the magnitudes of Hilbert Huang coefficients of other phases conforming that the fault type is BG fault on six phase transmission line with phase-B as the faulty phase. It can also be observed from Figure 8 that the HHT coefficient of phase-B has a lower magnitude of noise content in comparison to the noise content of HHT coefficients of other phases. This is due to the fact that the BG fault is a near-end fault which is

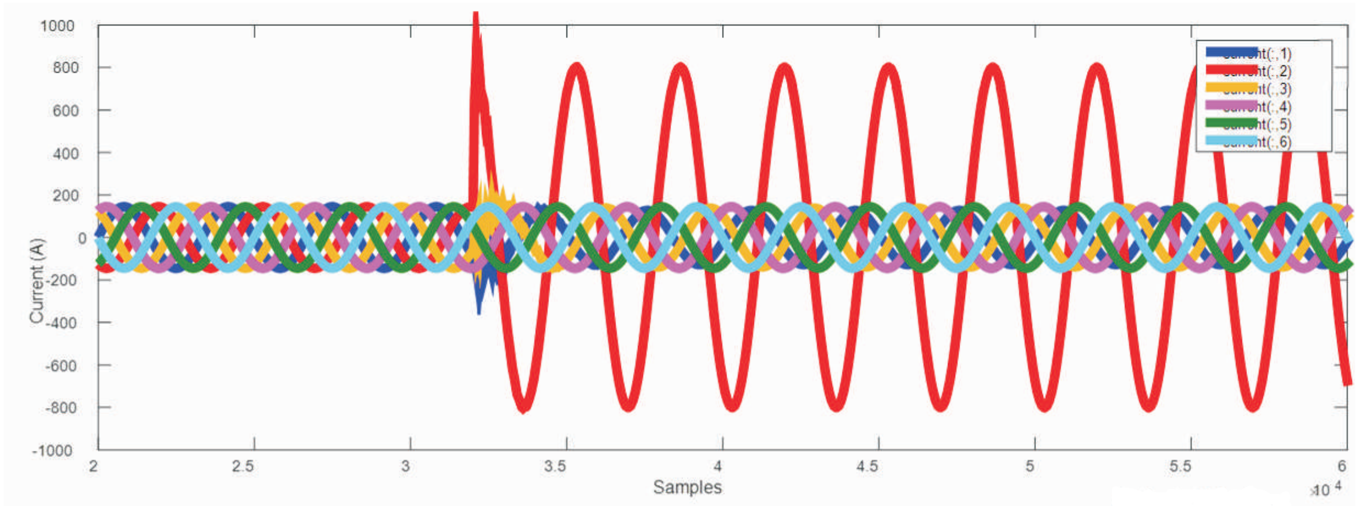

Figure 7. Six Phase Current during BG Fault at FIT=0.16 seconds at 4 km from bus-1 with RF = 6 Ω and RG = 9 Ω

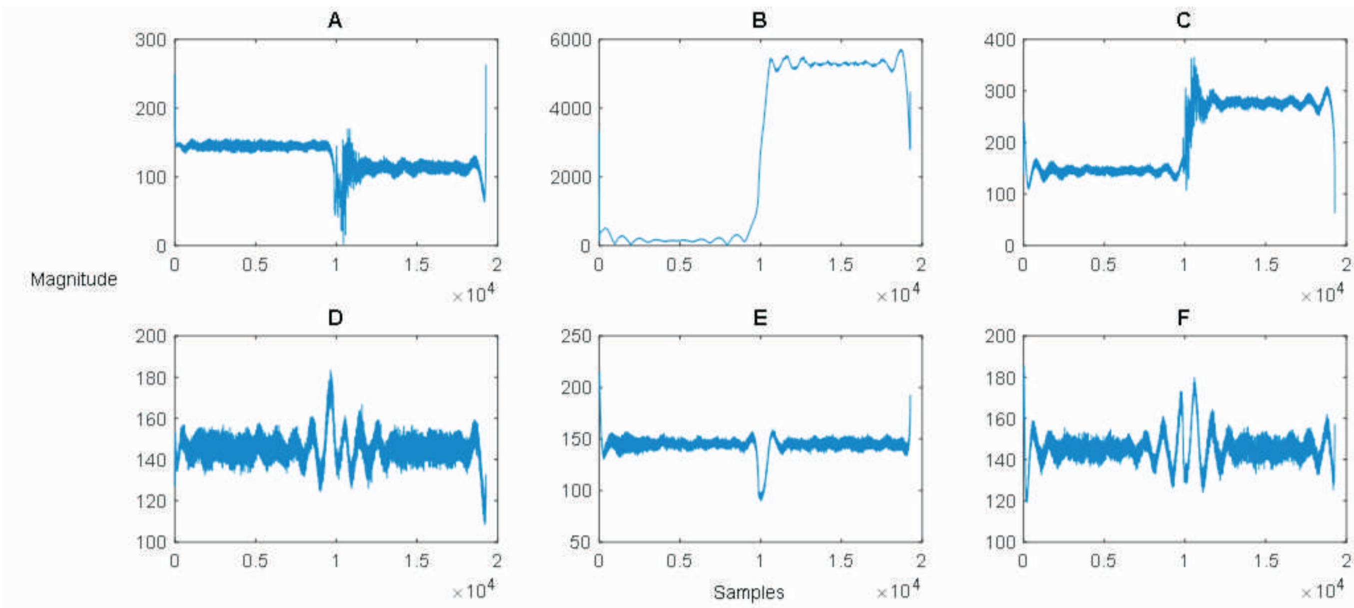

Figure 8. Hilbert Huang Transform Coefficients of Six Phase Current during BG fault at FIT=0.16 seconds at 4 km from bus-1 with RF = 6 Ω and RG = 9 Ω

simulated at a distance of 4 km from bus-1 on six phase transmission line. Table 3 depicts the response of proposed fault detection and classification technique for BG fault.

3.3 Performance in Case of CG near-end Fault: Case-III

The stability investigation of the proposed technique is evaluated for CG single line to ground fault when CG fault is triggered at a distance of 6 km which is near to the relaying point i.e. bus-1 at fault inception time of 0.025 seconds with RF = 9 Ω and RG = 12 Ω. Figure 9 demonstrates the waveform of six phase current when the CG fault is triggered at a distance of 6 km on six phase transmission line at FIT = 0.025 seconds. The process of feature

Phase	Hilbert Huang Transform Coefficients
A	263.5003
B	5.7108*10^3
C	365.8272
D	183.5112
E	214.9018
F	185.4333

Table 3. Test Result for BG Fault at 4 km from bus-1 at FIT = 0.16 seconds with RF = 6 Ω and RG = 9 Ω

extraction using the Hilbert Huang transform for six phase current during CG fault is depicted in Figure 10. Figure 10 shows the Hilbert Huang transform coefficients of six phase current during a CG fault at a distance of 6 km from the relaying point. As can be examined from Figure 10, the Hilbert Huang coefficient of phase C has a higher magnitude in comparison to the magnitudes of Hilbert Huang coefficients of other phases. This shows that the fault type is a CG fault on six phase transmission line with phase-C as the faulty phase. It can also be observed from Figure 10 that the HHT coefficient of phase-C has a lower magnitude of noise content in comparison to the noise content of HHT coefficients of other phases. This is due to the fact that the CG fault is a near-end fault which is simulated at a distance of 6 km from bus-1 on six phase transmission line. Table 4 depicts the response of proposed fault detection and classification technique for CG fault. It is clear from Table 4 that the proposed technique detects and classifies the fault accurately, for CG fault occurring very near to the relaying point of six phase transmission line.

3.4 Performance in Case of DG far-end Fault: Case-IV

The response of the proposed technique is evaluated for DG single line to ground fault when DG fault is triggered at a distance of 62 km away from the relaying point, i.e. from

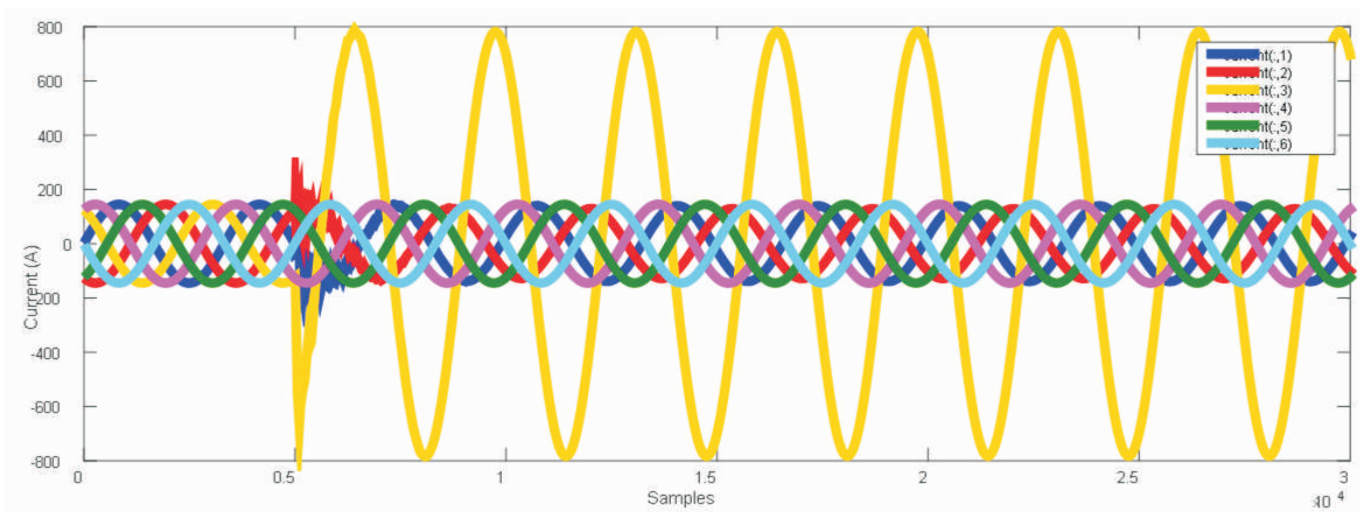

Figure 9. Six Phase Current during CG Fault at FIT=0.025 seconds at 6 km from bus-1 with RF = 9 Ω and RG = 12 Ω

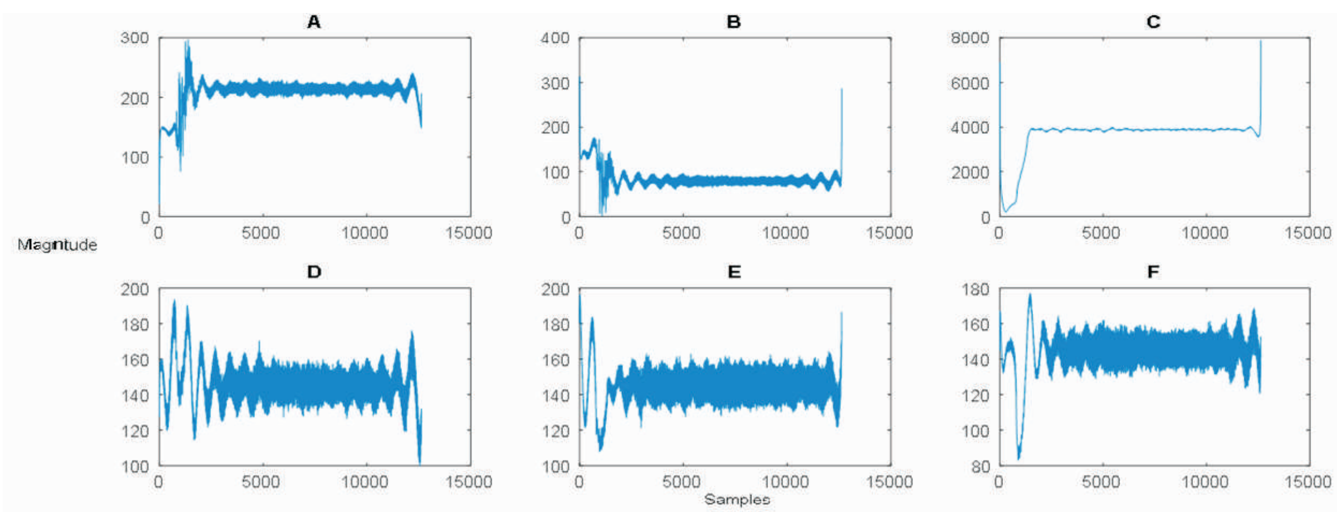

Figure 10. Hilbert Huang Transform Coefficients of Six Phase Current during CG Fault at FIT=0.025 seconds at 6 km from bus-1 with RF = 9 Ω and RG = 12 Ω

Phase	Hilbert Huang Transform Coefficients
A	297.0029
B	313.0387
C	7.8841*10^3
D	193.4840
E	196.2681
F	177.0821

Table 4. Test Result for CG Fault at 6 km from bus-1 at FIT= 0.025 seconds with RF = 9 Ω and RG = 12 Ω

bus-1 at fault inception time of 0.125 seconds with RF = 12 Ω and RG = 15 Ω. Figure 11 demonstrates the waveform of six phase current when the six phase transmission line is subjected to DG fault at a distance of 62 km away from the relay location at FIT = 0.125 seconds. The process of feature extraction using the Hilbert Huang transform for six phase current during DG fault is shown in Figure 12. Figure 12 depicts the Hilbert Huang transform coefficients of six phase current during DG fault at a distance of 62 km away from the relaying point. As can be seen from Figure 12, the Hilbert Huang coefficient of phase D has a higher magnitude in comparison to the magnitudes of Hilbert Huang coefficients of other phases conforming that the fault type is DG fault on six phase transmission line with phase-D as the faulty phase. It can also be observed in Figure 12 that the HHT coefficient of phase-D has a lower magnitude of noise content in comparison to the noise

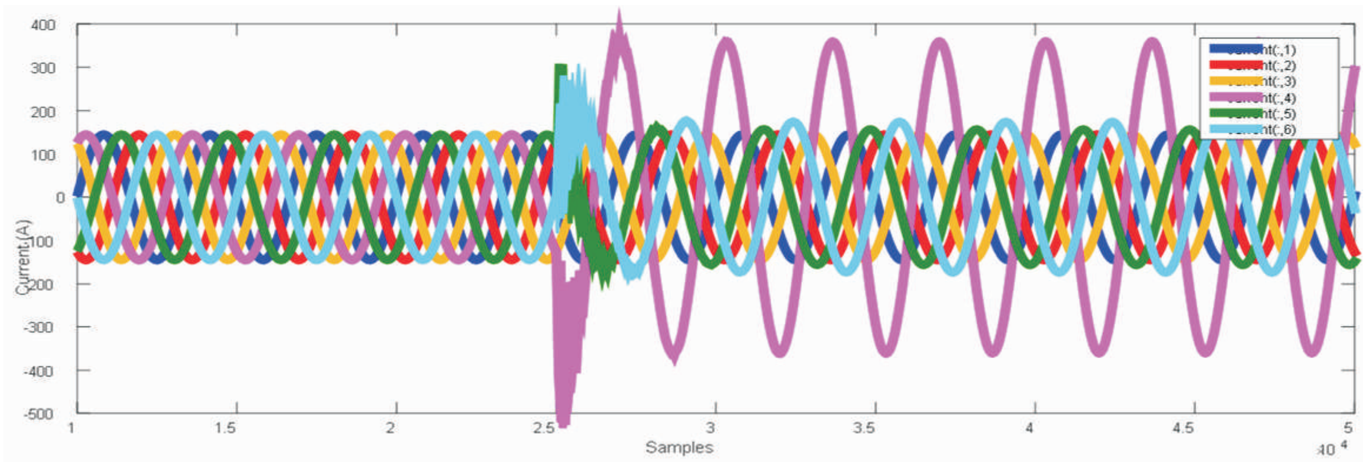

Figure 11. Six phase current during DG fault at FIT=0.125 seconds at 62 km from bus-1 with RF = 12 Ω and RG = 15 Ω

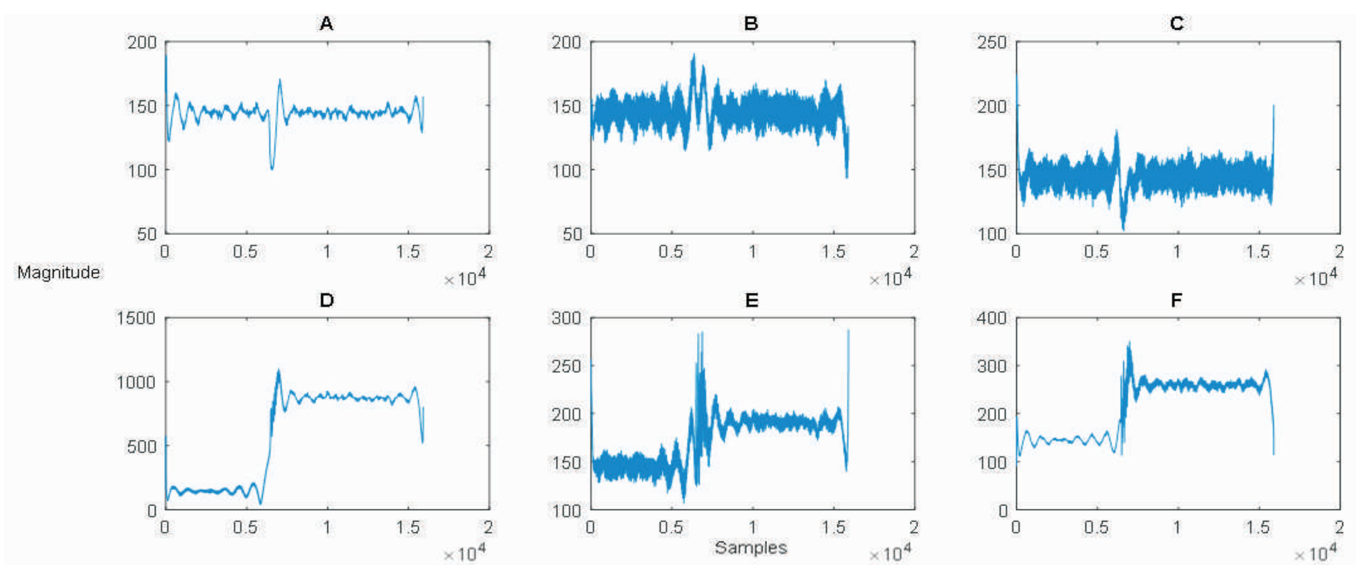

Figure 12. Hilbert Huang Transform Coefficients of Six Phase Current during DG fault at FIT=0.125 seconds at 62 km from bus-1 with RF = 12 Ω and RG = 15 Ω

content of HHT coefficients of other phases. This is due to the fact that the DG fault is a remote-end fault, which is simulated at a distance of 62 km from bus-1 on six phase transmission line. Table 5 depicts the response of proposed fault detection and classification technique for DG fault. It is clearly observed from Table 5 that the remote-end fault DG has been classified accurately.

3.5 Performance in Case of EG far-end Fault: Case-V

The stability investigation of the proposed technique is evaluated for EG single line to ground fault when EG fault is triggered at a distance of 64 km away from the relay location at fault inception time of 0.07 seconds with RF = 15 Ω and RG = 18 Ω. Figure 13 demonstrates the waveform of six phase current when the six phase transmission line is subjected to EG fault at 64 km away from the relay location at FIT = 0.07 seconds. The process of feature extraction using Hilbert Huang transform for six phase current during EG fault is depicted in Figure 14.

Phase	Hilbert Huang Transform Coefficients
A	189.4834
B	190.5874
C	224.1296
D	1.0998*10^3
E	287.3865
F	350.6758

Table 5. Test result for DG fault at 62 km from bus-1 at FIT= 0.125 seconds with RF = 12 Ω and RG = 15 Ω

Figure 14 demonstrates the Hilbert Huang transform coefficients of six phase current during EG fault at a distance of 64 km away from the relaying point. As can be seen from Figure 14, the Hilbert Huang coefficient of phase E has a higher magnitude in comparison to the magnitudes of Hilbert Huang coefficients of other phases. This exemplifies that the fault type is EG fault on six phase transmission line with phase-E as the faulty phase. It can also be observed in Figure 14 that the HHT coefficient of phase-E has a lower magnitude of noise content in comparison to the noise content of HHT coefficients of other phases. This is due to the fact that the EG fault is a far-end fault, which is simulated at a distance of 64 km from bus-1 on six phase transmission line. Table 6 depicts the response of proposed fault detection and classification technique for EG fault. It is clear from Table 6 that the proposed technique detects and classifies the fault correctly, for EG fault occurring far-away from the location of the relay of six phase transmission line.

3.6 Performance in Case of FG far-end Fault: Case-VI

The response of the proposed technique is evaluated for FG single line to ground fault when the FG fault is triggered at a distance of 66 km away from the relaying point at fault inception time of 0.045 seconds with RF = 18 Ω and RG = 21 Ω. Figure 15 demonstrates the waveform of six phase current when the six phase transmission line is subjected to FG fault at a distance of 66 km away from the relay location

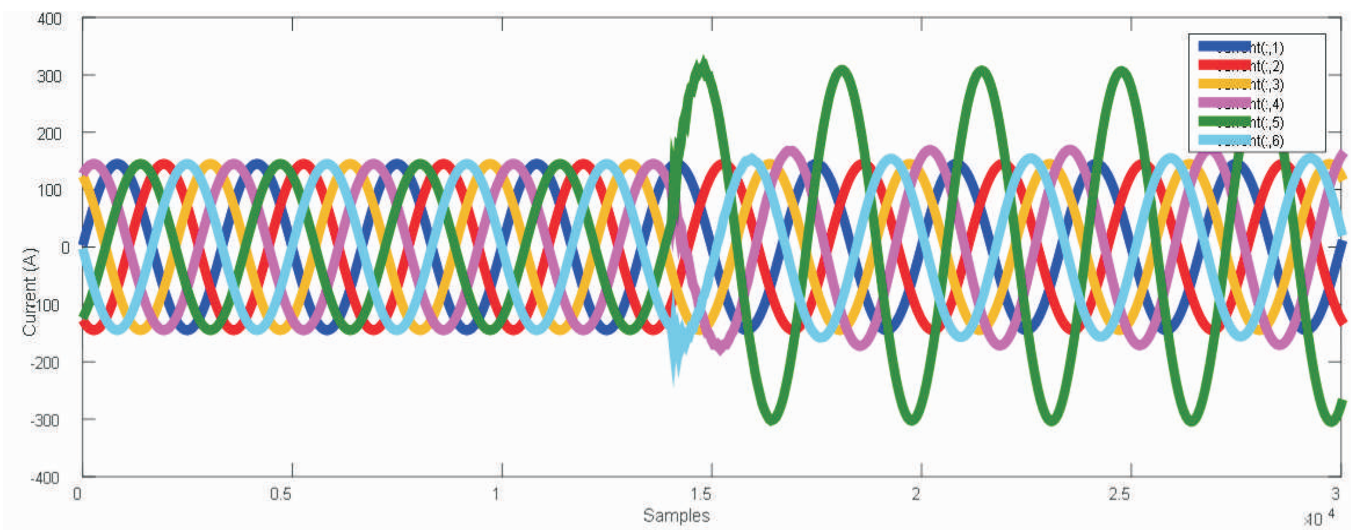

Figure 13. Six phase current during EG fault at FIT=0.07 seconds at 64 km from bus-1 with RF = 15 Ω and RG = 18 Ω

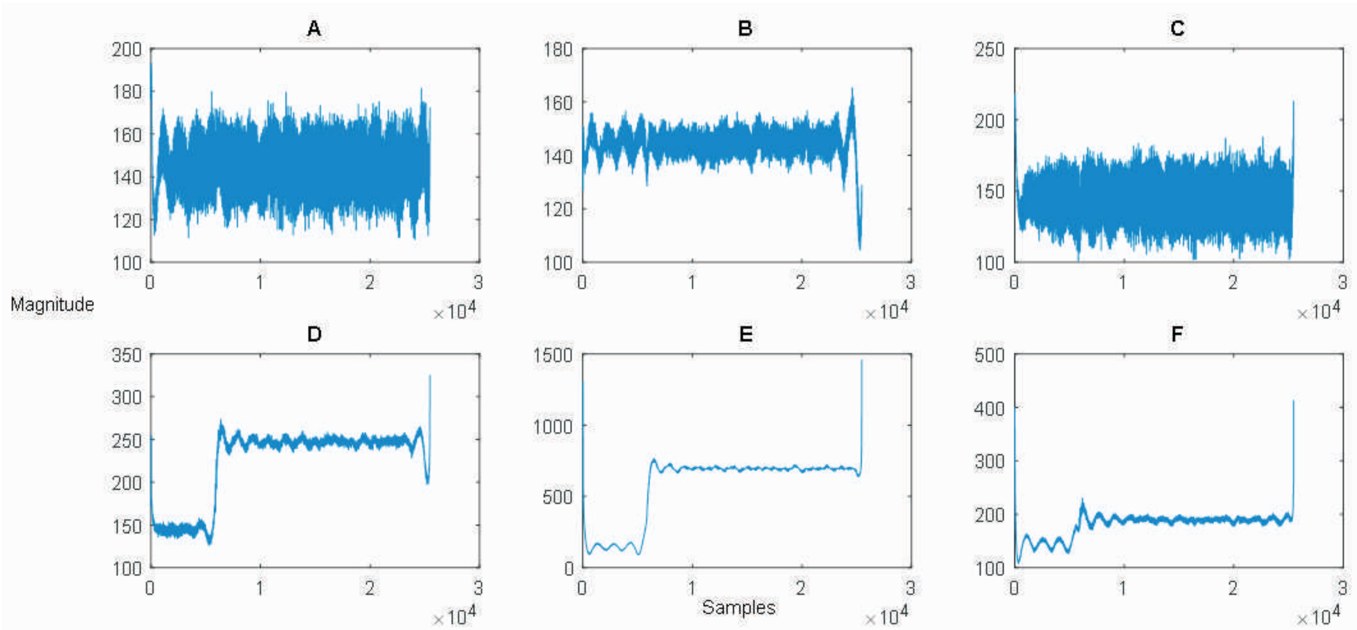

Figure 14. Hilbert Huang transform coefficients of six phase current during EG fault at FIT=0.07 seconds at 64 km from bus-1 with RF = 15 Ω and RG = 18 Ω

Phase	Hilbert Huang Transform Coefficients
A	193.1716
B	165.3308
C	218.2877
D	324.9550
E	1.4585*10^3
F	412.4476

Table 6. Test result for EG fault at 64 km from bus-1 at FIT=0.07 seconds with RF = 15 Ω and RG = 18 Ω

at FIT = 0.045 seconds. Figure 16 shows the procedure of feature extraction using the Hilbert Huang transform for six phase current during FG fault. Figure 16 depicts the Hilbert Huang transform coefficients of six phase current during FG fault at a distance of 66 km away from the relaying point. As can be seen from Figure 16, the Hilbert Huang coefficient of phase F has a higher magnitude in comparison to the magnitudes of Hilbert Huang coefficients of other phases conforming that the fault type is FG fault on six phase transmission line with phase-F as the faulty phase. It can

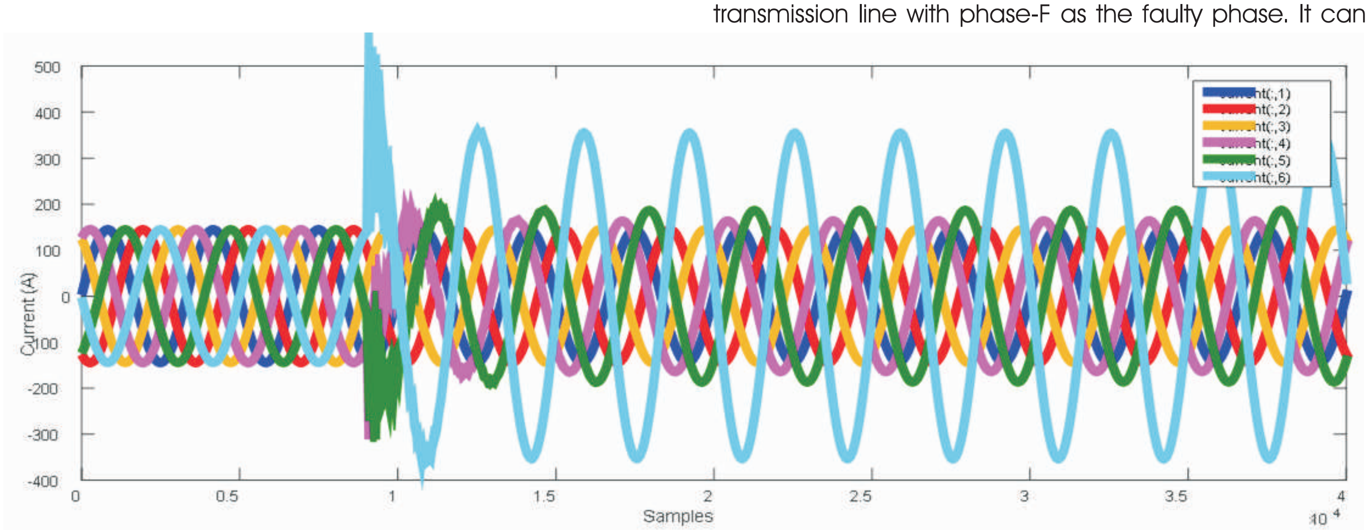

Figure 15. Six phase current during FG fault at FIT=0.045 seconds at 66 km from bus-1 with RF = 18 Ω and RG = 21 Ω

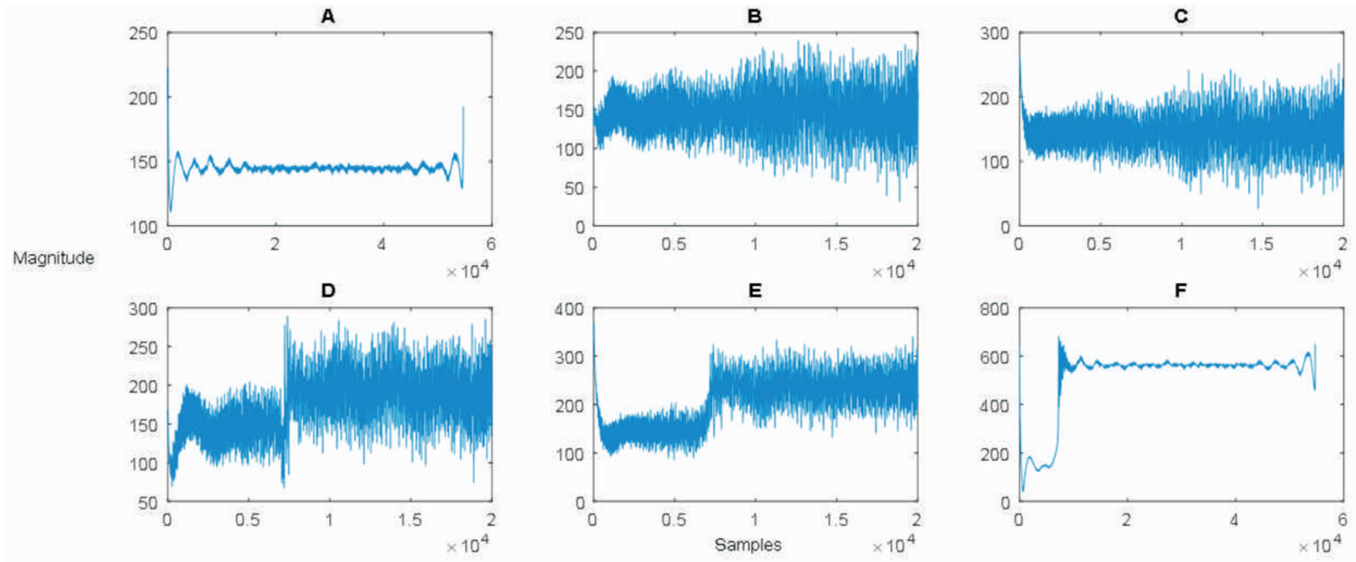

Figure 16. Hilbert Huang transform coefficients of six phase current during FG fault at FIT=0.045 seconds at 66 km from bus-1 with RF = 18 Ω and RG = 21 Ω

Phase	Hilbert Huang Transform Coefficients
A	223.0607
B	259.4662
C	267.1848
D	316.1225
E	378.8464
F	680.7636

Table 7. Test result for FG fault at 66 km from bus-1 at FIT=0.045 seconds with RF = 18 Ω and RG = 21 Ω

also be observed in Figure 16 that the HHT coefficient of phase-F has a lower magnitude of noise content in comparison to the noise content of HHT coefficients of other phases. This is due to the fact that the FG fault is a remote-end fault which is simulated at a distance of 66 km from bus-1 on six phase transmission line. Table 7 depicts the response of proposed fault detection and classification technique for FG fault. It is clearly observed from Table 7 that the remote-end fault FG has been classified accurately.

Conclusions

A new fault detection and faulty phase identification technique for six phase transmission line based on Hilbert Huang transform is presented which carries out the detection of single line to ground boundary faults and faulted phase identification concurrently. Faulted phase identification is carried out accurately. The main advantage of the proposed technique is that it uses only one side six phase fault current data. The effects of variations in the fault parameters, such as fault type, fault resistance, fault inception time, ground resistance, and fault location have been inspected on the performance of the proposed technique. The test results exemplify that the proposed technique effectively detects the single line to ground boundary faults in six phase transmission line.

References

[1]. **Ashok, V., & Yadav, A. (2018).** A relaying scheme for detection and classification of shunt faults in six phase transmission line based on DFT-FIS approach. *Journal of Power Technologies,* 98(2), 202-211.

[2]. **Binsaroor, A. S., & Tiwari, S. N. (1988).** Evaluation of twelve-phase (multiphase) transmission line parameters. *Electric Power Systems Research,* 15(1), 63-76.

[3]. **Demir, Z., Kilic, O., & Ozbey, S. (1998, May).** Calculation of load flow in mixed three-phase line and multiphase (six-phase and twelve-phase) line by the method of phase coordinate. In *Proceedings of the IEEE 6th International Conference on Optimization of Electrical and Electronics Equipments* (pp. 1-7). IEEE.

[4]. **Dorazio, T. F. (1990, April).** High phase order transmission. In *Proceedings of the IEEE Technical Conference on Southern Tier* (pp. 1-6). IEEE.

[5]. Fan, C., Liu, L., & Tian, Y. (2011). A fault location method for 12-phase transmission lines based on twelve sequence component method. *IEEE Transactions on Power Delivery,* 26(1), 135-142.

[6]. Gautam, N., Ali, S., & Kapoor, G. (2018, September). Detection of fault in series capacitor compensated double circuit transmission line using wavelet transform. In *Proceedings of the IEEE International Conference on Computing, Power and Communication Technologies (GUCON)* (pp. 769-773). IEEE

[7]. Gautam. N., Kapoor, G., & Ali, S. (2018). Wavelet transform based technique for fault detection and classification in a 400 kV double circuit transmission line. *Asian Journal of Electrical Sciences,* 7(2), 77-83.

[8]. Husain, Z., Singh, R. K., & Tiwari, S. N. (2007, May). Multi Phase (6-Phase and 12-Phase) Power Transmission Systems with TCSC. In *Proceedings of the WSEAS International Conference on Applications on Electrical Engineering* (pp. 246-250).

[9]. Kapoor, G. (2018a). A contemporary discrete wavelet transform based twelve phase series capacitor compensated transmission line protection. *International Journal of Engineering Research and Technology,* 7(5), 263-271.

[10]. Kapoor, G. (2018b). A discrete wavelet transform approach to fault location on a 138 kV two terminal transmission line using current signals of both ends. *ICTACT Journal of Microelectronics,* 4(3), 625-629.

[11]. Kapoor, G. (2018c). A fault location evaluation method of a 330 kV three phase transmission line by using discrete wavelet transform. *International Journal of Engineering Design and Analysis,* 1(1), 5-10.

[12]. Kapoor, G. (2018d). Detection of phase to phase faults and identification of faulty phases in series capacitor compensated six phase transmission line using the norm of wavelet transform. *i-managers Journal of Digital Signal Processing,* 6(1), 10-20.

[13]. Kapoor, G. (2018e). Discrete wavelet transform based technique to locate faults in three terminal transmission lines. *Journal of Advanced Research in Electrical Engineering and Technology,* 5(3), 1-8.

[14]. Kapoor, G. (2018g). Mathematical morphology based fault detector for protection of double circuit transmission line. *ICTACT Journal of MicroElectronics,* 4(2), 589-600.

[15]. Kapoor, G. (2018f). Fault detection of phase to phase fault in series capacitor compensated six phase transmission line using wavelet transform. *Jordan Journal of Electrical Engineering,* 4(3), 151-164.

[16]. Kapoor, G. (2018h). Protection scheme for double circuit transmission lines based on wavelet transform. *ICTACT Journal on Microelectronics,* 4(3), 656-664.

[17]. Kapoor, G. (2018i, September). Six phase transmission line boundary protection using mathematical morphology. In *Proceeding of the IEEE International Conference on Computing, Power and Communication Technologies (GUCON)* (pp. 857-861). IEEE

[18]. Kapoor, G. (2018j, December). Six phase transmission line boundary protection using wavelet transform. In *Proceedings of the 8th India IEEE International Conference on Power Electronics (IICPE).* IEEE.

[19]. Kapoor, G. (2018k). Wavelet transform based fault detector for protection of series capacitor compensated three phase transmission line. *International Journal of Engineering, Science and Technology (Africa),* 10(4), 29-49.

[20]. Kapoor, G. (2018l). Wavelet transform based detection and classification of multi-location three phase to ground faults in twelve phase transmission line. *Majlesi Journal of Mechatronic Systems,* 7(4), 47-60.

[21]. Kapoor, G. (2019a). A protection technique for series capacitor compensated 400 kV double circuit transmission line based on wavelet transform including inter-circuit and cross-country faults. *International Journal of Engineering, Science and Technology (Africa),* 11(2), 1-20.

[22]. Kapoor, G., Birla, D., & Tripathi, S. (2017). Discrete wavelet transform in series compensated transmission line for fault location. *International Journal of Electronics Electrical and Computational System,* 6(3), 110-115.

[23]. Kapoor, G. (2019b). Protection technique for series capacitor compensated three phase transmission line connected with distributed generation using discrete Walsh Hadamard transform. *International Journal of Engineering, Science and Technology (Africa),* 11(3), 1-10.

[24]. Koley, E., Verma, K., & Ghosh, S. (2017). A modular neuro-wavelet based non-unit protection scheme for zone identification and fault location in six phase transmission line. *Neural Compututing and Applications,* 28(6), 1369-1385.

[25]. Kumar, R., E. Koley, A. Yadav & A. S. Thoke (2014). Fault classification of phase to phase fault in six phase transmission line using HAAR wavelet and ANN. In *Proceedings of the IEEE International Conference on Signal Processing and Integrated Networks (SPIN)* (pp. 5-8).

[26]. Peng, X., Gang, W., Haifeng, L., Yuansheng, L., & Pu, Z. (2010, March). A new method for open conductors fault calculation of four-parallel transmission lines. In *Proceedings of the IEEE International Conference on Asia Pacific Power and Energy Engineering.* IEEE.

[27]. Sharma, P., Ali, S. & Kapoor, G. (2018a). Wavelet transform approach for fault detection of three phase transmission line compensated with series capacitor. *Asian Journal of Electrical Sciences,* 7(2), 8-13.

[28]. Sharma, P., Kapoor, G., & Ali, S. (2018b, September). Fault detection on series capacitor compensated transmission line using Walsh Hadamard transform. In *Proceedings of the IEEE International Conference on Computing, Power and Communication Technologies (GUCON)* (pp. 763-768). IEEE

[29]. Sharma, N., Ali, S., & Kapoor, G. (2018c, September). Fault detection in wind farm integrated series capacitor compensated transmission line using Hilbert Huang transform. In *Proceedings of the IEEE International Conference of the Computing, Power and Communication Technologies (GUCON)* (pp. 774-778).

[30]. Sharma, K., Ali, S., & Kapoor, G. (2018d). Six phase transmission line boundary fault detection using mathematical morphology. *International Journal of Engineering Research and Technology,* 6(12), 150-154.

[31]. Shukla, S. K., & Koley, E. (2017, December). Detection and classification of open conductor faults in six-phase transmission system using k- nearest neighbour algorithm. In *Proceedings of the 6th IEEE International Conference on Power Systems (ICPS)* (pp. 157-161). IEEE.

[32]. Soni, T., Ali, S., & Kapoor, G. (2017b). Wavelet transform based relaying scheme for double circuit transmission line protection. *International Journal of Engineering Research and Technology,* 6(8), 84-87.

[33].Soni, T., Ali, S. & Kapoor, G. (2017a). Discrete Wavelet Transform Based Fault Location in Double Circuit Transmission Line. *International Journal of Electronics Electrical and Computational System,* 6(3), 49-54.

[34]. Tripathi, V. K. & Bhardwaj, A. K. (2014). Investigation of multi phase power transmission system with thyristor controlled series capacitor. *International Journal of Innovative Research in Electrical, Electronics, Instrumentation and Control Engineering,* 2(6), 1572-1574.

[35]. Zhipeng, S., Pingping, W., Zheng, Y. & Xu, Z. (2012, March). Method for parameter decoupling for four-circuit transmission lines on the same tower. In *Proceedings of the IEEE International Conference on Asia Pacific Power and Energy Engineering Conference.* IEEE.

ABOUT THE AUTHOR

Gaurav Kapoor is currently working as an Assistant Professor in the Department of Electrical Engineering at Modi Institute of Technology, Kota, Rajasthan, India. He received his M.Tech. Degree in Power System Engineering from University College of Engineering, Rajasthan Technical University, Kota, Rajasthan, India in 2014. His research interests include Protection of Transmission Lines using Soft Computing Techniques.